

KOPIO SIGNAL in the case of: 1 γ PR + 1 γ CAL

1 Introduction

In the current design, the thickness of the Preradiator is 2.33 r.l. Thus, a photon has about an 83.6% chance to convert in the latter, and about 70% of the KOPIO signal events, have both photons converting before reaching the Calorimeter. The remaining 30% are/were considered less useful. In the case of only one gamma converting in the preradiator (PR+CAL), due to the absence of the directional information for another photon, and thus less constrained fit, it is harder to extract the signal (fraction of such events is roughly 27% of the total).

In the original KOPIO TDR (2001), it was argued, that about 30% of the regular case (2 γ 's converting in the Preradiator) event yield could be achieved. That meant that for a defined S/B ratio, the number of events with only 1 γ converting in the Preradiator is roughly one third of regular signal events with the same S/B. This statement was however made, when only half of the signal events had two photons converting in the Preradiator. If one were to simply apply the same rule of roughly 30% of the 2 γ in the Preradiator event yield, then it would mean that roughly third of the (PR+CAL) events could be extracted with the same S/B ratio. Quantitatively that means that PR+CAL case is expected to bring about $(0.3 \times 0.27 = 0.08)$ 8% of the total, or about 10% of the regular (both photons converted in the Preradiator) case.

However with thicker Preradiator, the rule of 30% may be misleading, and is utilized here only as a crude estimate. Due to worsened angular resolution, events with only one γ converting in the Preradiator could be even harder to separate from the background.

In this note an attempt to reevaluate the amount of signal events that could be extracted using the current model of the detector is undertaken.

2 FASTMC Assumptions

2.1 Geometry

Some of the detector's elements dimensions used in the FASTMC are presented in Table.2.1.

Beam divergence was $0.1 \text{ rad} \times 0.005 \text{ rad}$. For further details please refer to a geometry file `detector.23.dat`, which can be found in the `geometry` directory of the standard FASTMC code.

2.2 Photon Veto Assumption

One of the most influential characteristics of the KOPIO detector is the photon veto (PV) inefficiency. For our estimate, the so called 'TaskForce PV1' assumption was used.

Table 1: Dimensions of the detector elements, used in FASTMC study

Detector Element	X half dimension (cm)	Y half dimension (cm)	Z (cm)
BEAM PIPE	65	5	1015
DECAY VOLUME	160	160	400
PRERADIATOR	200	200	100
CALORIMETER	250	250	80
DS HOLE	110.25	11.55	180
CATCHER VOLUME	200	50	1120

The assumption is basically a synthesis of the “AvdS PV inefficiency” above 22 MeV and the “standard PV” below 22 MeV. The veto inefficiency versus γ ’s momentum is presented in Fig. 1.

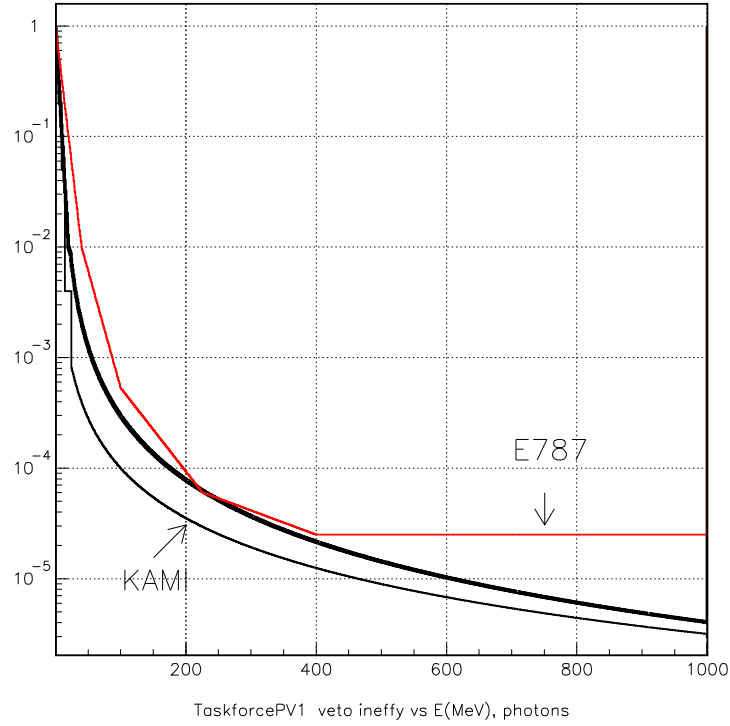
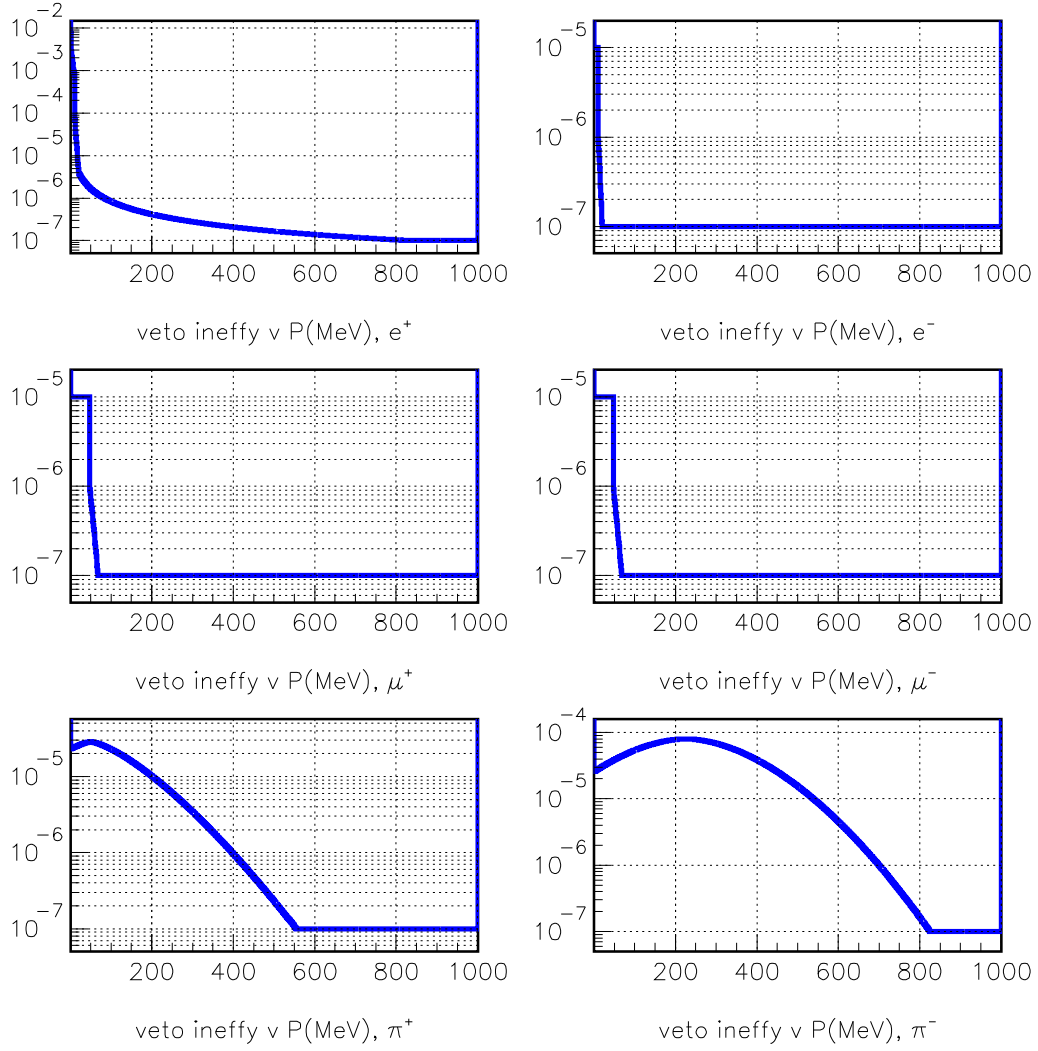


Figure 1: Photon Veto inefficiency (bold black curve) versus γ ’s momentum (MeV/c).

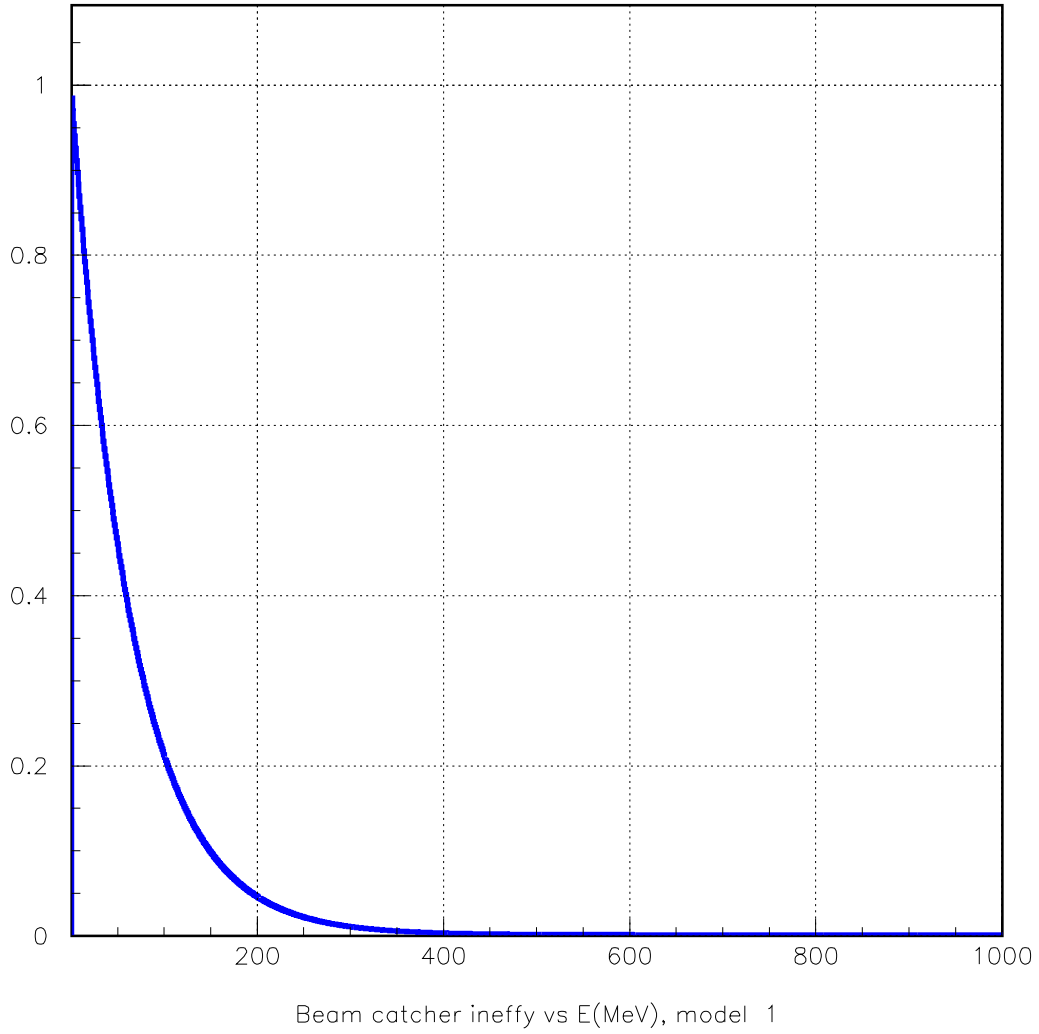
2.3 CPV

Charged particles veto (CPV) inefficiencies are presented below:



2.4 Catcher

The Beam Catcher inefficiency as a function of photon's momentum is presented below:



2.5 Resolution (smearing)

Energy resolution = $2.7\% / \sqrt{E(\text{GeV})}$

Coordinate and angular resolution in the Preradiator is approximated by the Bryman model.

For photons converting in the Calorimeter, spacial resolution is derived from the Shashlyk's granularity and is postulated as $11/\sqrt{12}$ cm. Effect of the calorimeter spacial resolution seems to be small, since event yields for standard cuts, are reduced only by a few percents ($\approx 4\%$).

The time resolution is assumed to be energy dependent $\approx 90\text{ps}/\sqrt{E(\text{GeV})}$ which is close to what was previously used (200 ps).

2.6 Reconstruction

Since one of the γ 's lacks directional information, the initial approximation for the vertex position is defined as an intercept of the trajectory of the Preradiator-converted photon with the horizontal ($Y=0$) plane (due to the horizontal profile of the KOPIO beam). Initial vertex position also gives approximation of the time at the vertex.

2.7 FastMC Results:

As a starting point, with no modification to the cuts, events with one gamma converting in the Preradiator and one in the Calorimeter, were generated and analyzed by the `anal.f` routine.

Some of the results can be seen below:

cut set	Kpnn	Kp2	Kcp3	Ke3g
Zcuts DSV	9.5 ± 0.1	5.2 ± 0.5	64.18 ± 33.3	6.8 ± 1.9
Jcuts DSV	36.4 ± 0.2	76.8 ± 12.3	172.3 ± 60.6	96.7 ± 8.4
AK prebasic	85.3 ± 0.4	3456 ± 1018	480804 ± 330503	179.7 ± 18.4
AK basic	18.1 ± 0.2	38.6 ± 12.3	107 ± 43	36.7 ± 4.7
AK loose	9.2 ± 0.1	5.9 ± 0.5	80.2 ± 38.3	18.6 ± 3.52
AK lominal	7.7 ± 0.1	4.0 ± 0.4	40.1 ± 27.5	14.2 ± 2.6
AK tight	5.4 ± 0.1	2.1 ± 0.2	2.4 ± 0.1	12.2 ± 2.4
AK tighter	3.35 ± 0.08	1.1 ± 0.2	0.92 ± 0.05	8.3 ± 2.1
AK tightest	2.46 ± 0.07	0.9 ± 0.2	0.4 ± 0.03	5.6 ± 1.7

The ke4 and the kp3 backgrounds rates were at the level of less then one event each. Knowing that AK cuts, especially "tighter" ones are fairly optimum, since they are representing the "clear" signal region, it is easy to assume that even with S/B=1 ratio, it would be hard to get more then a few signal events.

3 Likelihood application

3.1 Setup

Setup cuts, included:

fiducial cuts on the Z_{vertex} and P_{kaon}

Mpi0 mass cut relaxed to 50 MeV

David's cuts, supplemental to Andries's contour cut:

$L_{cut}(KE_{miss}) = y.gt.5. \quad .or. \quad P_{missMag}.lt.800.$

The general Likelihood function was constructed using the following 2-D variable correlations:

T^* vs $\text{Log}(E_{miss})$

E^* vs $\text{abs}(E_{g1^*} - E_{g2^*})$

Mpi0 vs E^*

Chi2 vs E^*

In addition one dimensional pdf was created for the vertex fit chi2.

3.2 Kp2 Background

The results for Kp2 background are presented in Fig. 2.

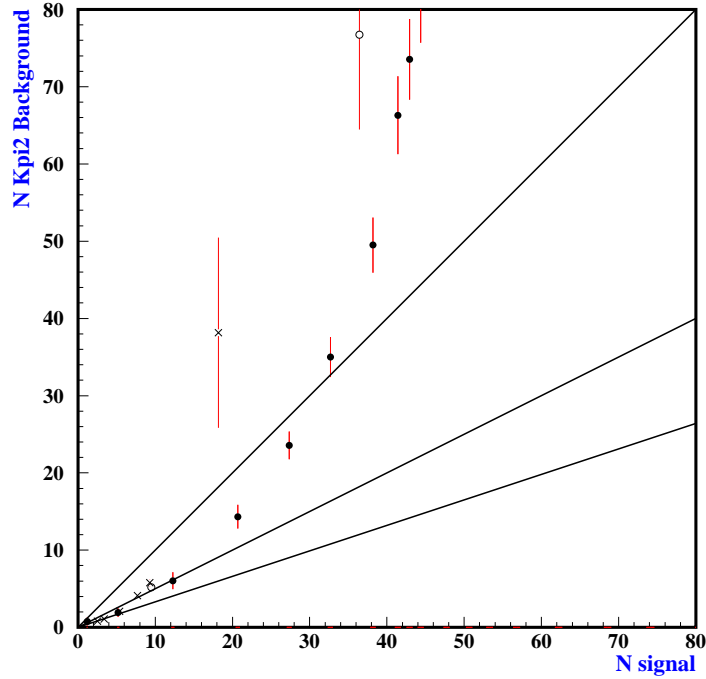


Figure 2: Number of Kp2 background events versus Kpnn signal events.. Circles represent Jcuts and Zcuts, while X's represent Akira's cuts.

Improvement over regular cuts is visible (almost a factor of 2).

Actual 2-D pdfs used in the likelihood for kp2 are presented in Fig.3.

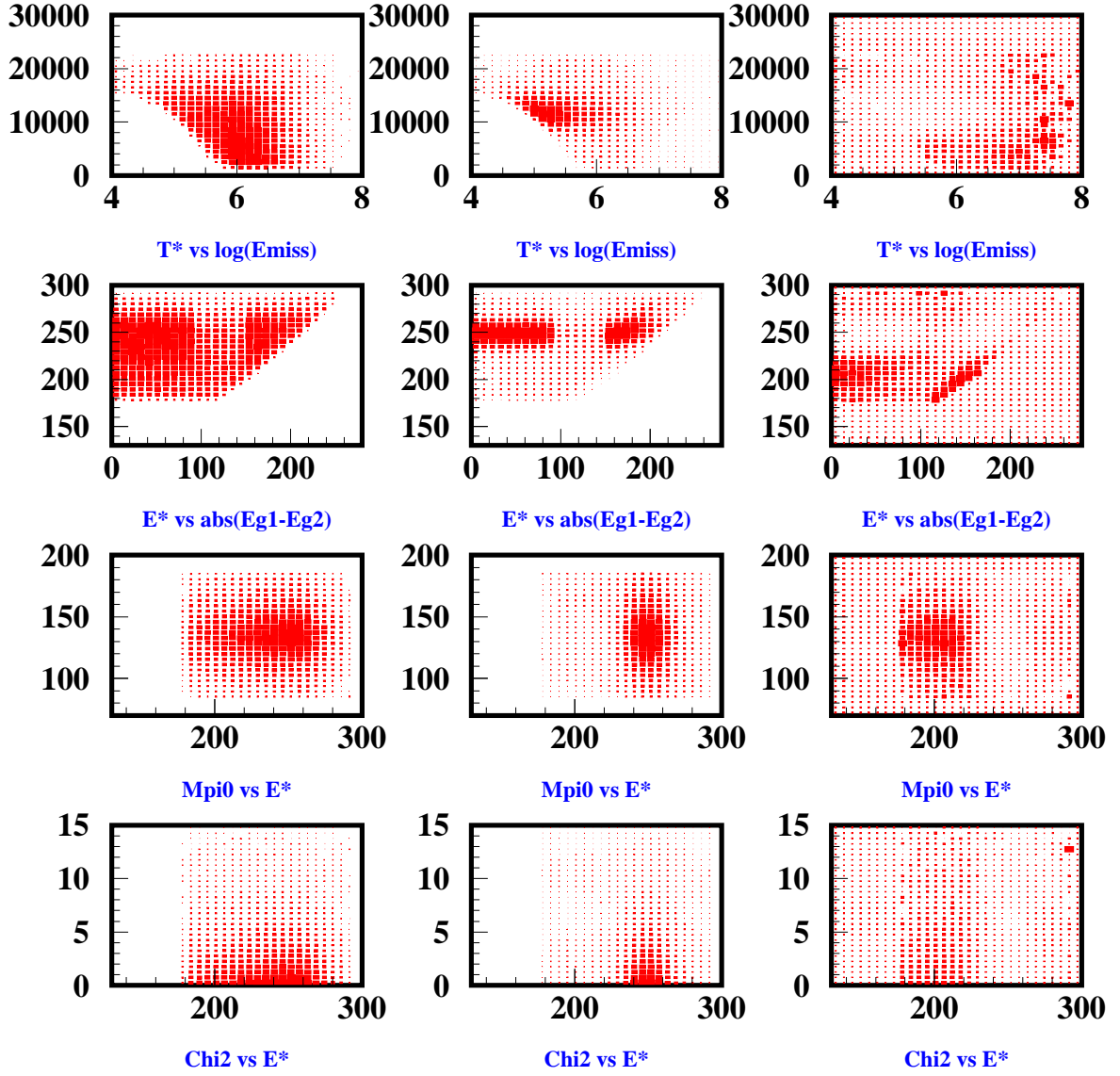


Figure 3: 2-D Distributions of the various kinematic variables for kpnn (left column), kp2 (center column) and S/B (right column)

3.3 Kcp3 Background

Since the Kcp3 background appeared to be large, the likelihood was used to suppress it. Results can be seen in Fig. 4. Note: only the Kcp3 background is considered. Results are excellent, but only the Kcp3 background was considered. Problem is that

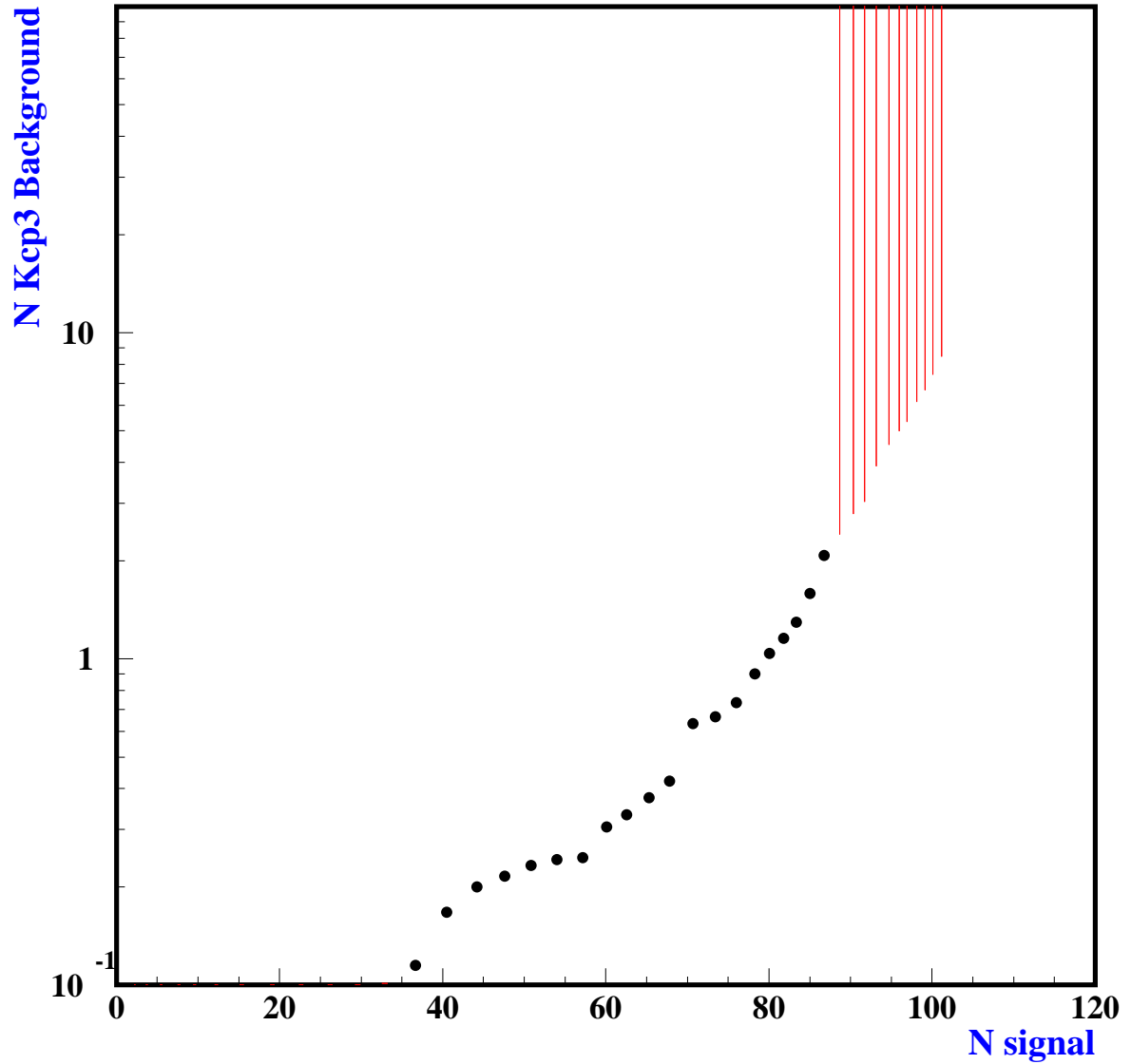


Figure 4: Number of Kcp3 background events versus Number of signal events

“Kcp3 background free” regions can overlap with the Kp2 background regions.

Actual 2-D pdfs used in the likelihood for Kcp3 are presented in Fig. 5.

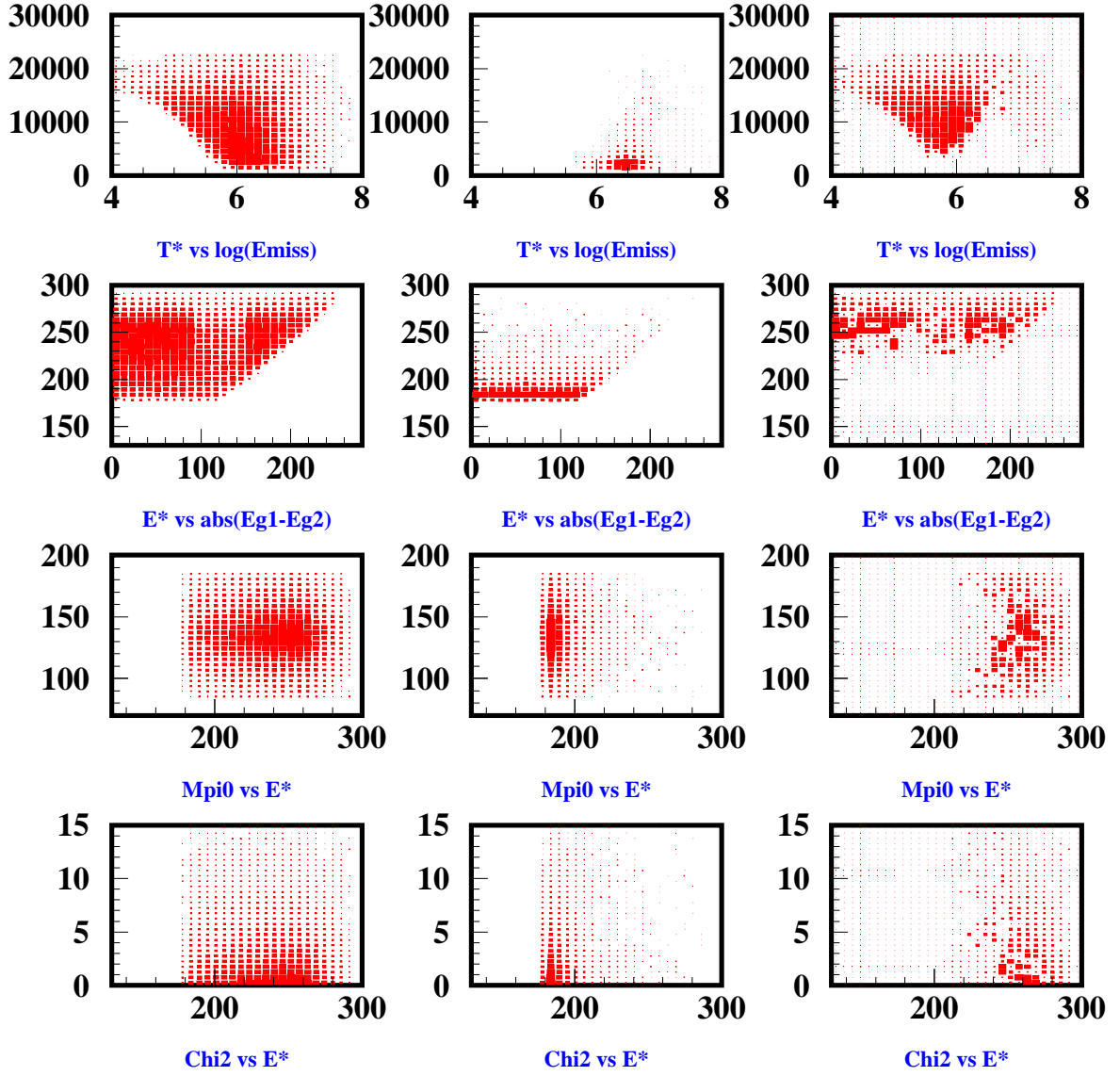


Figure 5: 2-D Distributions of the various kinematic variables for kpn (left column), kcp3 (center column) and S/B (right column)

3.4 Ke3g Background

Another largely contributing background comes from the radiative Ke3. Again, considering only this background likelihood method is tested and results can be seen in Fig. 6

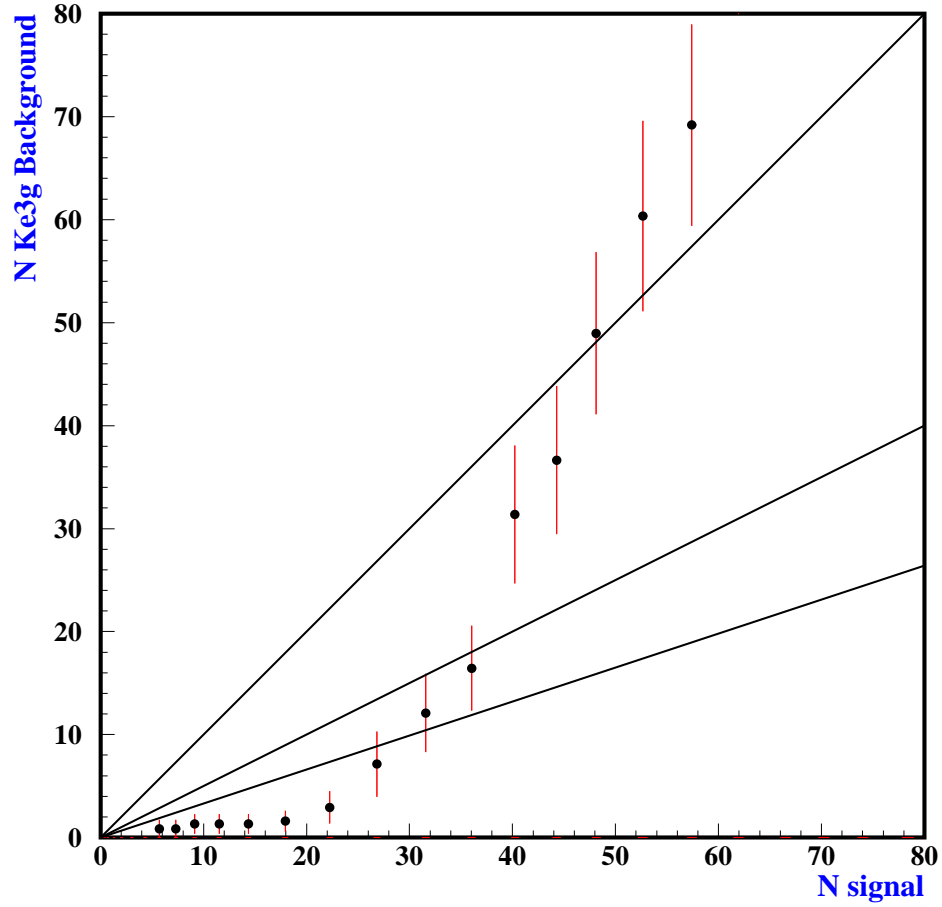


Figure 6: Number of Ke3g background events, versus number of signal events

Actual 2-D pdfs used in the likelihood for Ke3g are presented in Fig. 7

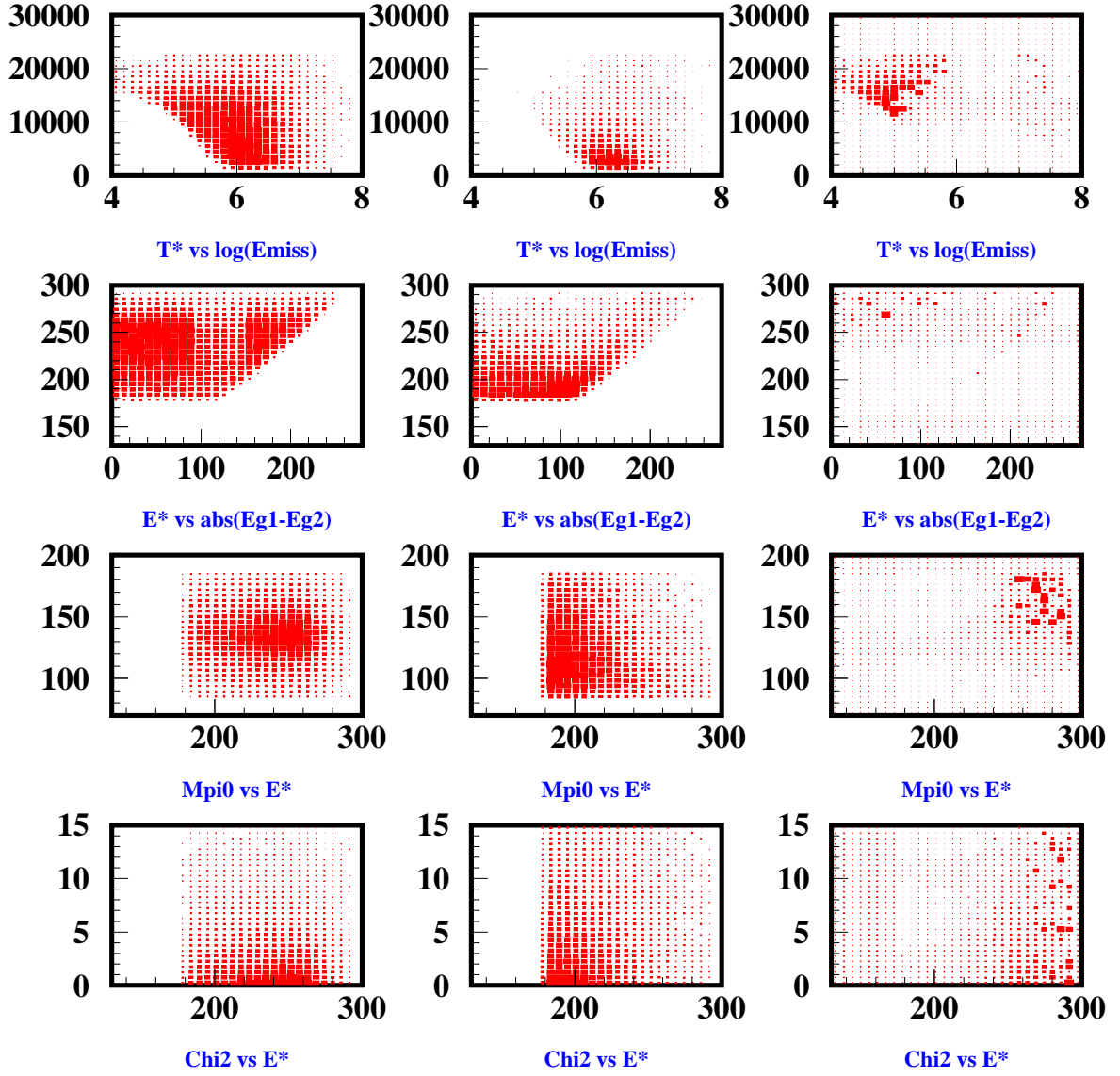


Figure 7: 2-D Distributions of the various kinematic variables for kpn (left column), ke3g (center column) and S/B (right column)

4 Combining major backgrounds

Although Likelihood proved to be very useful in fighting major backgrounds **INDIVIDUALLY**, it is more important to assess its power when backgrounds are combined. For this purpose, pdfs were formed for each background (kp2,kcp3,ke3g) and then added proportionally to their contribution (no of expected events) to form a general background pdfs.

Results werent very satisfying and can be seen in Fig.8, while actual general pdfs can be seen in Fig.9. Even S/B of 1 could not be achieved. This troubling result should be however further investigated, since obviously poorer reconstruction is not inherent to all events of this type. Thus by finding a good criteria to reject poorly reconstructed events, one could improve the signal yield.

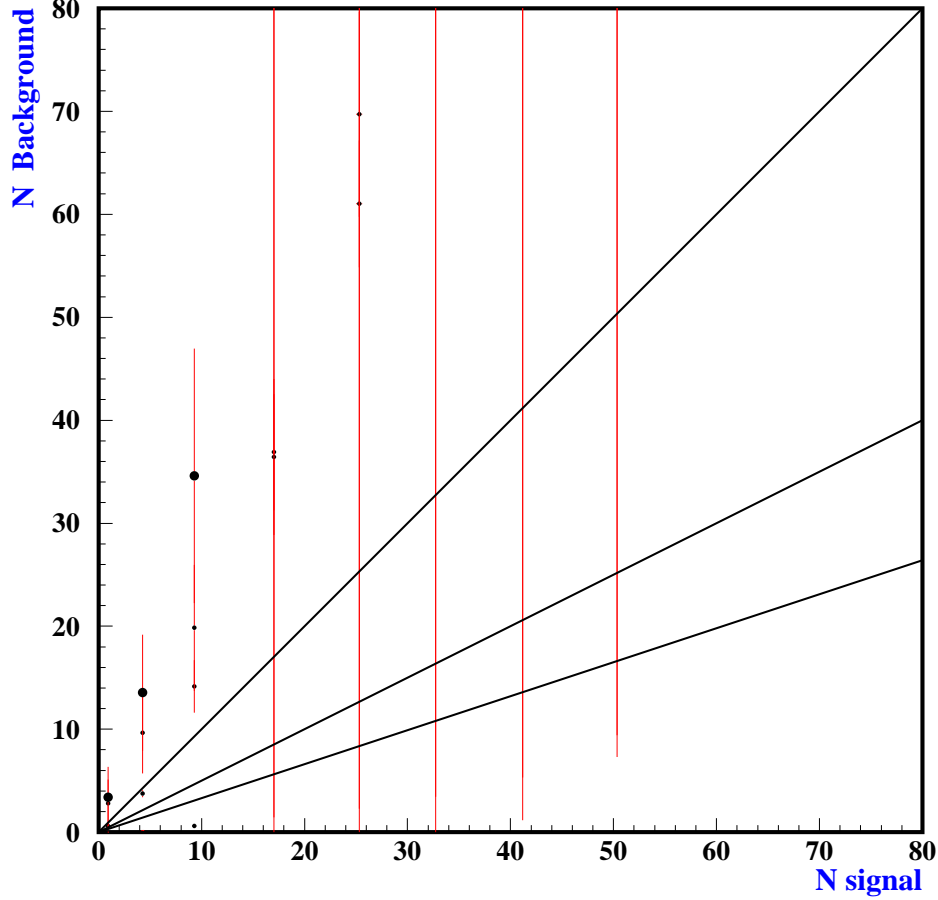


Figure 8: Number of Ke3g background events, versus number of signal events

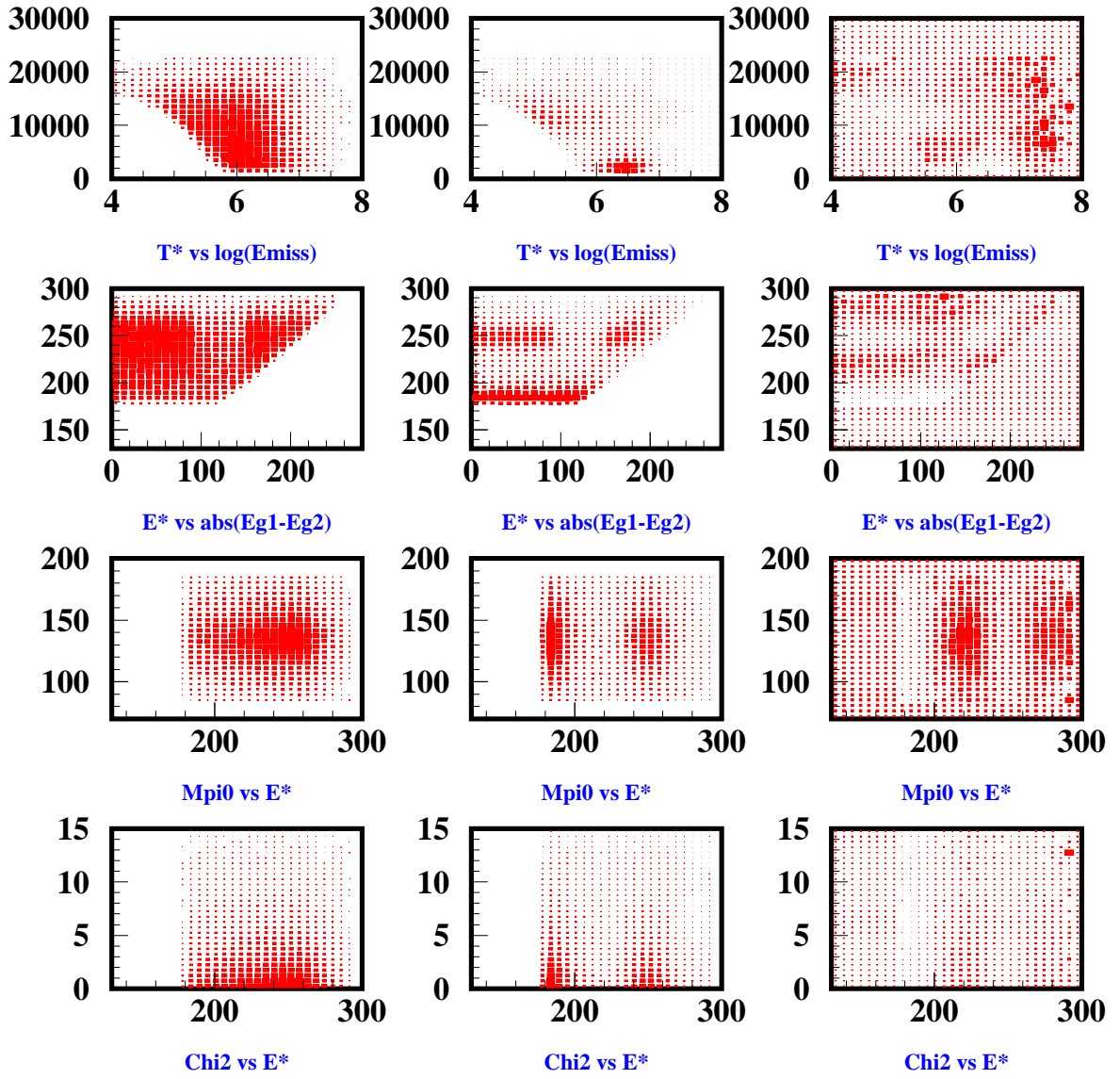


Figure 9: 2-D Distributions of the various kinematic variables for kpn (left column), ke3g (center column) and S/B (right column)

5 Finding Quality Estimator

One would rightfully assume, that quality of the reconstruction depends on the quality of the vertex, and in the case of the 1g in PR is dominated by the angle of the preradiator converted photon. As a possible quality gauge, a $\tan \theta$ of the preradiator converted photon could be used.

to be continued on saturday...

P.S. θ seems to work, since with about 60% loss in signal, improvement in M_{π^0} resolution is good, and almost at the level of normal case (2gPR) events